Journal of Fluorescence (2019) 29:1161–1170
https://doi.org/10.1007/s10895-019-02432-x

ORIGINAL ARTICLE

Spectral-Fluorescent Study of the Interaction of Cationic and Anionic Polymethine Dyes with Sodium Deoxycholate in Aqueous Solutions

Pavel G. Pronkin[1] · Alexander Tatikolov[1] · Ina Panova[2]

Received: 17 June 2019 / Accepted: 27 August 2019 / Published online: 4 September 2019

Abstract

The noncovalent interaction of a number of cationic and anionic *meso*-substituted polymethine (carbocyanine) dyes with sodium deoxycholate (NaDC) as a biologically important surfactant was studied by spectral-fluorescent methods. The following dyes were studied: 3,3′-di(β-hydroxyethyl)-9-methylthiacarbocyanine-iodide (K1), 3,3′-di(β-hydroxyethyl)-5,5′-dimethoxy-9-ethylthiacarbocyanine iodide (K2), 3,3′,9-trimethylthiacarbocyanine iodide (K3, Cyan 2), 3,3′-di(γ-sulfopropyl)-9-methylthiacarbocyanine-betaine (A1), and 3,3′-di(γ-sulfopropyl)-4,5,4′,5′-dibenzo-9-ethylthiacarbocyanine-betaine (A2, DEC). Upon addition of increasing concentrations of NaDC, the absorption spectra of dyes K1–K3 in aqueous solutions exhibit changes due to the formation of dye aggregates and their subsequent decomposition into monomers. The formation of aggregates of K1–K3 leads to broadening of the absorption spectra and an appearance of additional bands. Upon binding to the surfactant, the *cis*-monomers of the dyes undergo partial *cis–trans* conversion, which is accompanied by an increase in the fluorescence intensity. The binding constants of the dyes to NaDC were estimated on the basis of Scatchard and Hill models from the dependences of the absorption and fluorescence spectra on the concentration of NaDC.

Keywords Polymethine (cyanine) dyes · Sodium deoxycholate · Micelles · Fluorescent probes · *cis–trans* conversion · Aggregation

Introduction

Polymethine (cyanine) dyes possess a unique set of photophysical and photochemical properties, which determine the broad scope of applications of these compounds [1]. The high sensitivity of polymethine dyes to the properties of the molecular microenvironment makes it possible to use them as spectral-fluorescent probes for biomacromolecules and for biological imaging [2, 3]. A number of works were devoted to studying the photophysics of polymethine dyes in normal and reverse micelles formed from various types of synthetic surfactants [4–7]. In addition to synthetic surfactants, there is a large class of biologically important natural surfactants – bile salts (BS, or cholates), the structure of which differs significantly from that of synthetic surfactants. Cholate molecules have a steroid skeleton, the concave side of which is hydrophilic due to the presence of OH groups, and the convex side with angular methyl groups is hydrophobic [8]. When BS concentration increases above a critical value, micelles begin to form: initially primary micelles are formed due to hydrophobic interactions between the convex regions of the molecules (with an aggregation number of 2–10), and then secondary micelles are formed due to hydrogen bonding between primary micelle associates (with an aggregation number of 10–100). Hence, a number of authors identify for BS two values of critical micelle concentrations

Electronic supplementary material The online version of this article (https://doi.org/10.1007/s10895-019-02432-x) contains supplementary material, which is available to authorized users.

✉ Pavel G. Pronkin
pronkinp@gmail.com

✉ Alexander Tatikolov
tatikolov@mail.ru

[1] N.M. Emanuel Institute of Biochemical Physics, Russian Academy of Sciences, Kosygin St. 4, Moscow 119334, Russia

[2] N.K. Koltsov Institute of Developmental Biology, Russian Academy of Sciences, Vavilov St. 26, Moscow 119334, Russia

(CMC): CMC1 and CMC2 for primary and secondary micelles, respectively [9–12].

In a number of works, systems containing BS were studied by the method of spectral-fluorescent probes using xanthene and benzophenoxazine dyes [13, 14]. At present, the interaction of polymethine dyes with BS is not sufficiently studied (only qualitative data were obtained) [15]. Photochemical processes in two polymethine dyes in BS micellar systems were studied in [16].

In this work, the noncovalent interaction of polymethine dyes with BS was studied by spectral-fluorescent methods in more detail, with estimating the binding constants. As objects of the study, a number of *meso*-substituted thiacarbocyanines and sodium deoxycholate (NaDC) as BS were chosen (see Fig. 1): the cationic carbocyanines 3,3′-di(β-hydroxyethyl)-9-methylthiacarbocyanine chloride (K1), 3,3′-di(β-hydroxyethyl)-5,5′-dimethoxy-9-ethylthiacarbocyanine chloride (K2), 3,3′,9-trimethylthiacarbocyanine iodide (K3, or Cyan 2, previously studied in [15]), and the anionic dyes 3,3′-di(γ-sulfopropyl)-9-methylthiacarbocyanine betaine (A1) and 3,3′-di(γ-sulfopropyl)-4,5,4′,5′-dibenzo-9-ethylthiacarbocyanine betaine (A2, DEC in [15]). The binding constants of the dyes to NaDC were estimated.

Experimental

Materials

Tiacarbocyanine dyes K1, K2, A1 and A2 were obtained from Prof. B.I. Shapiro (Research Institute "Khimfotoproekt", Moscow), and dye K3 from Prof. C.M. Yarmoluk (Institute of Molecular Biology and Genetics, National Academy of Sciences of Ukraine). Sodium deoxycholate (NaDC) was commercially available (Sigma–Aldrich). Distilled water was used as a solvent.

Analysis Methods and Equipment

The absorption spectra were measured on an SF-2000 spectrophotometer (Russia), and the fluorescence spectra on a Fluorat-02-Panorama spectrofluorimeter (Russia), using quartz semi-microcells. The fluorescence excitation spectra were corrected for the sample transmission and the spectral characteristic of the excitation channel.

The fluorescence quantum yields (φ_{fl}) of dyes K1 and K2 were determined by comparison with a standard, 3,3`-diethylthiacarbocyanine iodide (DTC, $\varphi_{fl(st)} = 5\%$ in methanol [17]), using Eq. (1):

$$\varphi_{fl} = \frac{(1-T_{st})F}{(1-T)F_{st}}\frac{n^2}{n_{st}^2}\varphi_{fl(st)} \approx \frac{F}{F_{st}}\varphi_{fl(st)} \quad (1)$$

where T_{st} and T are the transmittances of the standard and dye solutions, respectively, at the excitation wavelength; F_{st} and F are the integrals of the emission bands of the standard and the dye, respectively; and n_{st} and n are the refraction indexes of the standard and dye solutions respectively ($n \approx n_{st}$ for the same solvents) [18]. Under the experimental conditions, $T \approx T_{st}$; the experimental error was ±10%. The fluorescence quantum yields of other dyes were determined earlier [19, 20].

The measurements were carried out at a temperature of 22 ± 2°C.

The deconvolution of the absorption spectra of the dyes into components corresponding to the monomeric forms and aggregates was carried out using the iterative procedure [21].

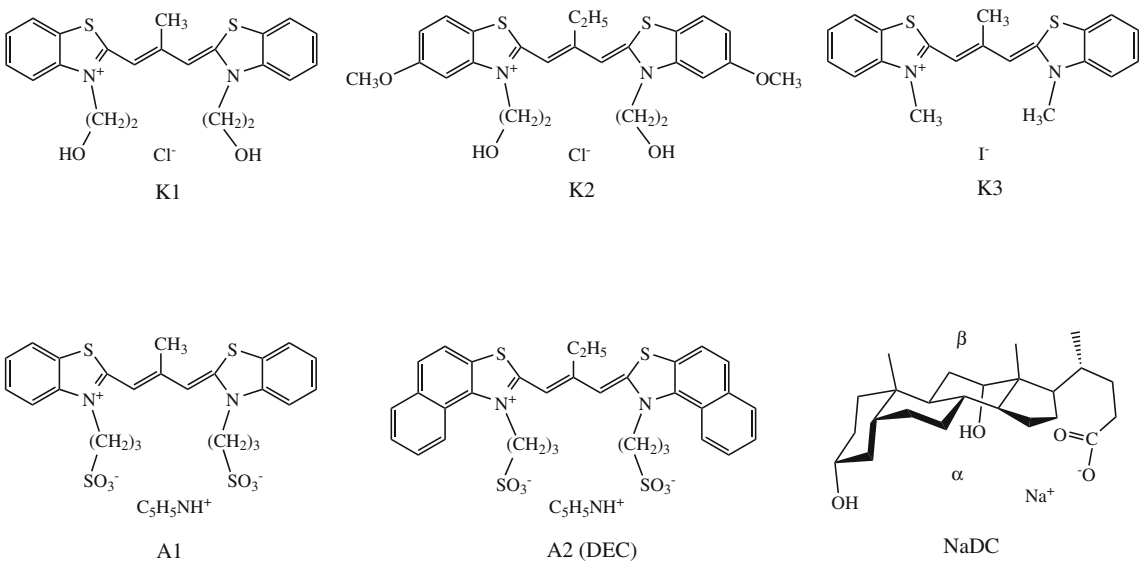

Fig. 1 Structures of studied compounds

Results and Discussion

Spectral-Fluorescent Properties of the Dyes in Aqueous Solutions

In aqueous solutions, the *meso*-substituted thiacarbocyanines K1–K3 are present mainly in the monomeric (M) form. In the absorption spectra, the M bands of K1–K3 have a short-wavelength vibronic shoulder at about 500 nm typical for cyanine dyes. Due to their hydrophobic properties, K1–K3 tend to form unstructured aggregates in aqueous solutions; the contribution of the aggregate absorption leads to some broadening of the absorption spectral bands. In aqueous solutions, cyanines under study have low fluorescence quantum yields (see Table 1 and [19, 20]). The maxima of the fluorescence excitation spectra of K1–K3 and A1 are bathochromically shifted with respect to those of the absorption spectra (see Table 1). The anionic dye A1 in an aqueous solution is present in the monomeric form, and a single band is observed in the fluorescence spectrum of A1.

It is known that *meso*-substituted cyanines in solutions are in the form of *cis*- and *trans*- isomers, being in equilibrium, which depends on the solvent polarity. In polar solvents the equilibrium is shifted toward *cis*-isomers, whereas in nonpolar ones to *trans*-isomers. The isomers differ in their spectral-fluorescent properties [23, 24]. In particular, *cis*-isomers of thiacarbocyanine dyes absorb at shorter wavelengths than *trans*-isomers, (for example, the *trans*-isomer of K3 has $\lambda_{abs}^{max} \sim 547$ nm, while the *cis*-isomer has $\lambda_{abs}^{max} = 535$ nm [19]). In addition, the *trans*-isomers of the dyes possess fluorescence, while the *cis*-isomers practically do not fluoresce.

The low fluorescence quantum yields and the discrepancy between the absorption and excitation spectra are due to the presence of the dyes in aqueous solutions mainly in the form of nonfluorescent *cis*-isomers (*trans*-isomers are present in trace quantities).

The anionic dye A2 (DEC) is also characterized by an equilibrium between *cis*- and *trans*-isomers; in addition, this dye in aqueous solutions is prone to dimerization. At $c_{A2} \sim 1$–2 μM, the dye is present mainly in the dimer (D) form with $\lambda_{abs}^{max} = 535$ nm, which is in equilibrium with M (in the form of the *cis*-isomer). The absorbance of the *cis*-monomer in the absorption spectra corresponds to the M-shoulder with $\lambda_{abs}^{max} \sim 575$ nm [6, 7]. The effects of isomeric equilibrium and aggregation determine the weak fluorescence of A2 in aqueous solutions, which is caused by the presence of traces of the *trans*-isomer (the fluorescence excitation spectrum with $\lambda_{ex}^{max} \sim 595$ nm), whereas the *cis*-isomer and the dimer of A2 do not fluoresce [6, 7, 22].

Interaction of the Cationic Dyes K1–K3 with NaDC

Upon the introduction of NaDC into aqueous solutions of K1 and K2 ($c_{K1} \approx c_{K2} = 1$–2 μM), changes in the spectra are observed, which are explained by the noncovalent interaction of dye molecules with the surfactant (similar changes were observed upon the introduction of cholates into an aqueous solution of K3 [15]). In the region of relatively low concentrations of NaDC $c_{NaDC} \sim 1$–2 mM < CMC1 (for NaDC, CMC1 and CMC2 are 2.4 and 6.5 mM, respectively [11, 12]), a decrease in the intensity of the bands of dye *cis*-monomers is observed in the absorption spectra. In the case of K1, the decrease in the absorption band is accompanied by its broadening and a bathochromic shift of the maximum (see Figs. 2, 3; $\Delta\lambda_{abs}^{max} \sim 4$ nm). At $c_{NaDC} = 2.4$ mM, an additional short-wavelength shoulder appears in the K2 absorption spectra ($\lambda_{abs}^{max} \sim 535$–540 nm; see Electronic Supplementary Material). The main absorption band of K2 also shifts to the long-wavelength region ($\Delta\lambda_{abs}^{max} \sim 12$ nm; see Electronic Supplementary Material).

Similar effects were observed in the case of K3: at $c_{NaDC} \sim 1$ mM, the initial absorption band of the dye decreases and broadens with the appearance of a short-wavelength shoulder in the spectra [15]. These changes indicate the presence of aggregates of the dyes, which are formed on NaDC molecules.

The aggregates of K1 and K2, formed in the presence of NaDC, as those of K3 [15], emit fluorescence with a broad spectrum, the maximum of which lies in the long-wavelength region ($\lambda_{fl}^{max} \sim 630$–660 nm) and the excitation spectrum is shifted to the short-wavelength side with respect to the absorption bands of the M forms of the dyes. Therefore, these aggregates can be attributed to H-aggregates of the dyes. In

Table 1 Maxima of the absorption (λ_{abs}^{max}), fluorescence (λ_{fl}^{max}) and fluorescence excitation (λ_{ex}^{max}) spectra, as well as Stokes shifts ($\Delta\lambda^{Stokes} = \lambda_{fl}^{max} - \lambda_{abs}^{max}$), differences between the maxima of the excitation and absorption spectra ($\Delta\lambda^{max} = \lambda_{ex}^{max} - \lambda_{abs}^{max}$), and fluorescence quantum yields (φ_{fl}) for dyes K1–K3 and A1, A2 in aqueous solutions

Dye	λ_{abs}^{max}, nm	λ_{fl}^{max}, nm	$\Delta\lambda^{Stokes}$, nm	λ_{ex}^{max}, nm	$\Delta\lambda^{max}$, nm	φ_{fl}, %	Ref.
K1	544	566	22	551	7	0.20	This work
K2	563	586	23	573	10	0.15	
K3	535	564	29	548	13	0.30	[19]
A1	542	556	14	548	6	0.64	[20]
A2	535 (dimer), ~575 (*cis*-M)	623	~48	595	~20		[6, 7, 22]

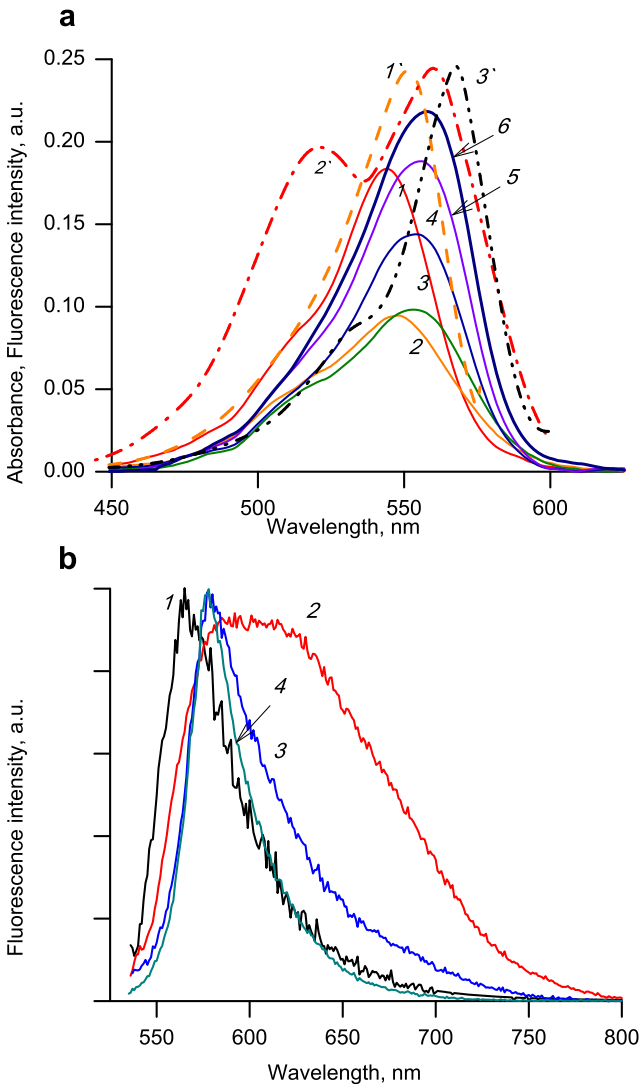

Fig. 2 **a** Absorption (solid lines *1*–*6*) and normalized fluorescence excitation spectra (dashed lines *1′*–*3′*) of dye K1 (c_{K1} = 1.8 μM) at various concentrations of NaDC: (*1*, *1′*, λ_{reg} = 585 nm) 0, (*2*, *2′*, λ_{reg} = 630 nm) 2.17, (*3*) 5.46, (*4*, *3′*, λ_{reg} = 610 nm) 10.1, (*5*) 22.4, and (*6*) 78.0 mM; (**b**) normalized fluorescence spectra of K1 (λ_{ex} = 525 nm) at (*1*) 0, (*2*) 2.17, (*3*) 5.47, and (*4*) 12.6 mM NaDC

particular, the maximum of the fluorescence excitation spectrum of the aggregates of K1 λ_{ex}^{max} = 521 nm (see Fig. 2), and in the case of K3 λ_{ex}^{max} = 490 nm, with the Stokes shift being as high as 130–170 nm.

An increase in NaDC concentration leads to decomposition of the aggregates of K1–K3 into monomeric molecules. In the absorption spectra of K1 and K2, the aggregate bands disappear at c_{NaDC} ~ 4.0 mM (i.e., at c_{NaDC} < CMC2 = 6.5 mM); simultaneously the M band of the dyes grows, and its bathochromic shift increases. For example, in the case of K1 and K2, the most dramatic spectral changes occur in the NaDC concentration range from 0 to ~5 mM (see Fig. 2). For K3, the aggregates begin to decompose into dye monomers bound to the surfactant at c_{NaDC} > 6 mM. A growth in the monomer absorption band (λ_{abs}^{max} = 545–550 nm) and an

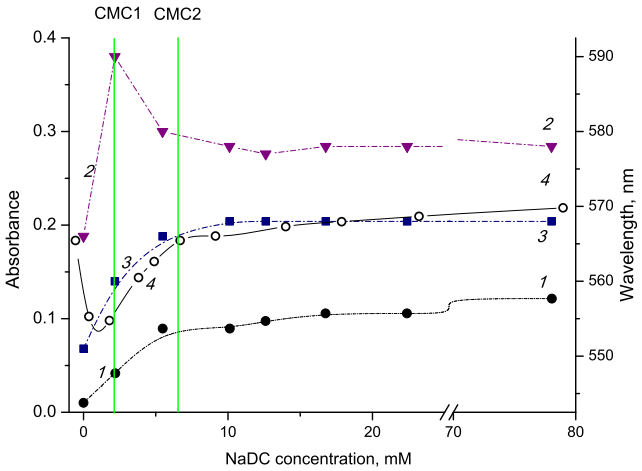

Fig. 3 Dependences of (*1*–*3*) the positions of the maxima of the (*1*) absorption, (*2*) fluorescence, (*3*) fluorescence excitation spectra, and (*4*) the absorbance at the absorption maximum of dye K1 on the concentration of NaDC. The CMC values are marked with vertical green lines

increase in the fluorescence intensity (λ_{fl}^{max} = 576 nm) are observed in the spectra, which correspond to the monomeric dye K3 associated with the surfactant [15]. Fig. 4a shows the results of deconvolution of the absorption spectra of dye K3 into Gaussian components (monomers and aggregates), and Fig. 4b shows the changes in the intensities of the absorption bands of the aggregates and the monomeric dye molecules under the action of NaDC.

The fluorescence intensity (I_{fl}) of dyes K1–K3 in the presence of NaDC increases significantly: for K2 at c_{NaDC} = 3.92 mM, I_{fl}/I_{fl0} = 14. Since dyes K1–K3 without NaDC are in the *cis*-form (with trace amounts of the *trans*-isomer), the appearance and growth of the *trans*-isomer upon the addition of NaDC (Fig. 4b) indicates partial *cis*–*trans* conversion occurring upon binding of the dyes to NaDC. The fluorescence quantum yields of the *trans*-isomers of the cationic cyanines associated with NaDC may increase as a result of spatial fixation of fragments of dye molecules, which leads to a decrease in the rates of internal conversion and an increase in the quantum yield of fluorescence as a competing process. At the same time, the absorption spectra of the monomers of dyes K1–K3 remain broader than the fluorescence excitation spectra measured at the same concentrations of NaDC (at c_{NaDC} > CMC2 = 6.5 mM). This indicates simultaneous binding to NaDC of the *trans*- (fluorescent) and *cis*- (nonfluorescent) isomers of the dyes.

The data of Fig. 4b clearly show changes in the dye state in a solution with increasing surfactant concentration: conversion of initial (*cis*) monomers of K3 into aggregates at relatively low surfactant concentrations (some monomers remain in the solution), which decompose into monomers at higher surfactant concentrations. The latter process is accompanied by partial *cis*–*trans* isomerization of the dye.

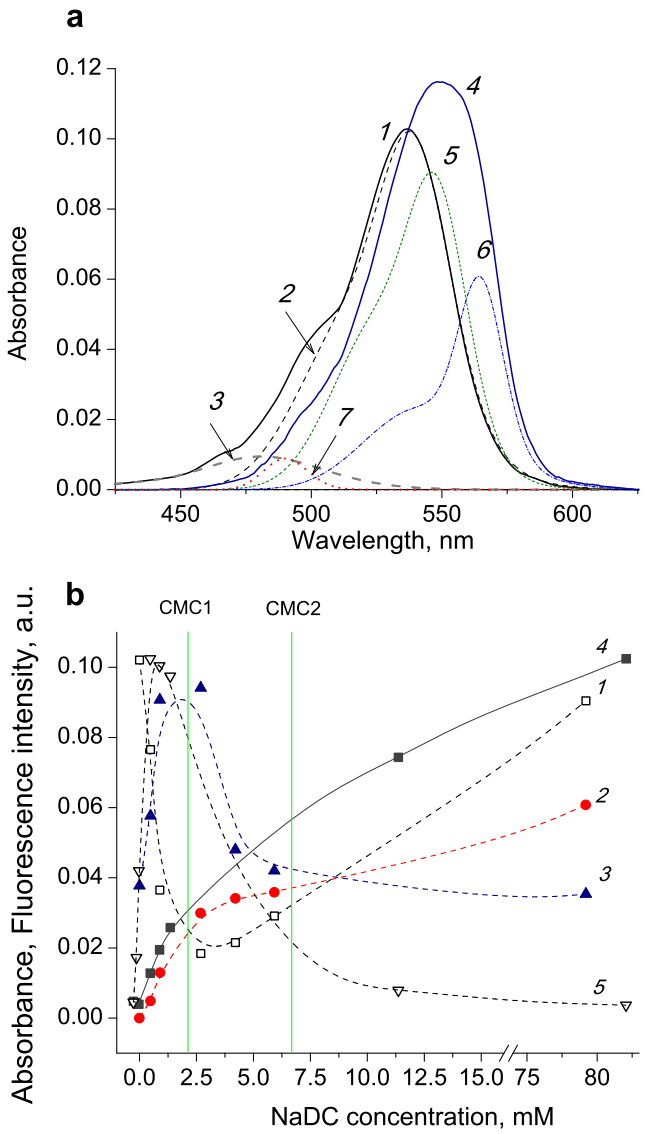

Fig 4. (a) (*1*, *4*) Absorption spectra of K3 and (*2*, *3*, *5*–*7*) their deconvolution components in the (*1*–*3*) absence and (*4*–*7*) presence of NaDC (79.2 mM): (*2*, *5*) *cis*-isomer, (*6*) *trans*-isomer, and (*3*, *7*) aggregates of dye K3. (b) Dependences of (*1*–*3*) the maximum absorbances of (*1*) *cis*-isomer, (*2*) *trans*-isomer, and (*3*) aggregates of K3; fluorescence intensity of (*4*) *trans*-monomer and (*5*) aggregates of K3 on the concentration of NaDC. The CMC values are marked with vertical green lines

The phenomena observed may be explained as follows. The interaction of carbocyanine dyes with NaDC occurs noncovalently due to Coulomb forces and hydrophobic interactions. For cationic dyes K1–K3, both Coulomb and hydrophobic forces lead to attractive interaction between the dye and surfactant molecules. This results in the formation of dye–surfactant associates (dye aggregates on surfactant templates) even at low surfactant concentrations (<CMC1). With increasing the surfactant concentration (up to ~CMC2 and above), high concentration of formed micelles with strong hydrophobic interaction with dye molecules leads to decomposition of dye aggregates to form associates of monomeric dyes with micelles. The interaction with the surfactant also leads to a certain *cis–trans* shift of the isomeric equilibrium and binding of both (*cis* and *trans*) isomers to micelles. Since, unlike *cis*-isomers, *trans*-isomers of *meso*-substituted thiacarbocyanine dyes have fluorescence, the *cis*→*trans* conversion leads to growing fluorescence. This may be due to lowering polarity of molecular microenvironment of a dye molecule on binding to a micelle, because for *meso*-substituted thiacarbocyanine dyes a decrease in the solvent polarity results in a shift of the *cis–trans* equilibrium toward the *trans*-isomer [15].

Interaction of the Anionic Dyes A1 and A2 with NaDC

When small amounts of NaDC (c_{NaDC} about CMC1) were introduced into an aqueous solution of the anionic dye A1 ($c_{A1} = 1.2$ μM), no noticeable changes were observed in the absorption or fluorescence spectra. This shows the absence of the interaction of the dye with molecules and small micelles of NaDC. With an increase in the surfactant concentration above CMC2, a long-wavelength shift of the maximum of the absorption spectrum of A1 is observed (see Fig. 5): at $c_{NaDC} =$ 30 mM $\Delta\lambda_{abs}^{max} \sim 9$ nm. In the fluorescence spectrum of A1, $\lambda_{fl}^{max} \sim 578$ nm (Fig. 5, curves *2*, *7*), and the fluorescence intensity increases: at $c_{NaDC} \sim 8$ mM $I_{fl}/I_{fl0} = 3.7$; at $c_{NaDC} = 30$ mM $I_{fl}/I_{fl0} = 14$. The position of the maximum of the fluorescence excitation spectrum does not coincide with that of the absorption spectrum and is shifted bathochromically ($\lambda_{ex}^{max} = 567$ nm, whereas $\lambda_{abs}^{max} = 551$ nm, at the maximum surfactant concentration $c_{NaDC} = 30$ mM).

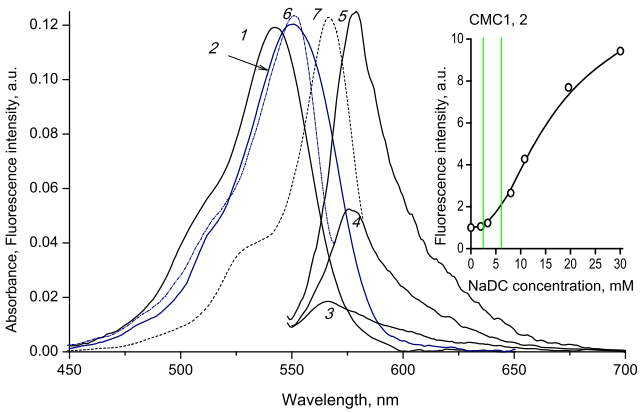

Fig. 5 (*1*, *2*) Absorption, (*3*–*5*) fluorescence ($\lambda_{ex} = 540$ nm), and (*6*, *7*) fluorescence excitation ($\lambda_{reg} = 590$ nm) spectra of dye A1 ($c_{A1} = 1.3$ μM) at different concentrations of NaDC: (*1*, *3*, *6*) 0, (*4*) 10.8, and (*2*, *5*, *7*) 30 mM. Inset: change in the fluorescence intensity of A1 as a function of NaDC concentration. The CMC values are marked with vertical green lines

When increasing concentrations of NaDC are introduced into a solution of A2 (c_{A2} = 1–2 μM), changes in the absorption spectra due to the decomposition of dye dimers into *cis*-monomers (λ^{abs}_{max} ~ 580 nm) begin at low surfactant concentrations ($c_{NaDC} \approx$ CMC1 = 2.4 mM) and continue to CMC2 [15]. The fluorescence intensity of A2 increases due to conversion of the dye into the *trans*-isomer. The main fluorescence growth begins at surfactant concentrations above CMC1; the fluorescence growth continues even at surfactant concentrations much higher than CMC2 [15].

In the case of the interaction of anionic dyes A1 and A2 with anionic NaDC, to form a dye–surfactant complex, the contribution of hydrophobic interactions should exceed the effect of electrostatic repulsion. For A1, no noticeable spectral-fluorescent changes occur at [NaDC] ≤ CMC1, and only at surfactant concentrations in the region of CMC2 the changes due to the *cis–trans* conversion are observed. This means that the energy of hydrophobic interaction of A1 with molecules and smaller (primary) micelles of NaDC is insufficient for overcoming the electrostatic repulsion upon the formation of the complex. However, this energy is sufficient for larger (secondary) NaDC micelles. For A2, which is mainly present in the dimeric form in aqueous solutions, the energy of hydrophobic interactions with molecules and small micelles of NaDC (at [NaDC] ≤ CMC1) is enough for a shift of the dimer–monomer equilibrium (Eq. (8)) toward the monomer (in the *cis* form). As for K1–K3, the interaction of the dyes with secondary micelles (at [NaDC] ~ CMC2 and above) leads to partial conversion of the *cis*-isomers into the *trans* form. The lowering micropolarity may be also the reason for the *cis*→*trans* conversion observed for dyes A1 and A2 [15] even at very high surfactant concentrations (>> CMC2), which is due to rearrangement of secondary micelles (probably related to their enlargement).

Estimation of the Association Constants of the Dyes with NaDC

The results obtained show that the interaction of the dyes with NaDC leads to a partial *cis–trans* conversion, which is accompanied by the fluorescence growth. For cationic dyes K1–K3, the processes of the interaction with NaDC include the formation of aggregates (at low concentrations of the surfactant) and their decomposition (at higher concentrations of the surfactant). As a consequence, modeling of the interaction of the dye with the surfactant for estimation of the association constant is complicated and possible only with some simplifications. As can be seen from above, dyes K1–K3, as well as A1, in dilute aqueous solutions are present mainly in the form of monomers, and the aggregates of K1–K3 are formed as intermediates at low NaDC concentrations, which then, with growing surfactant concentration, decompose into monomers associated with the surfactant (A1 does not form aggregates). If we neglect the intermediate formation of the aggregates and assume that the monomers (M) of dyes K1–K3, as A1, immediately bind to the surfactant micelles $(nS)_{mic}$, then for these dyes we obtain the following simplified scheme:

$$M + (nS)_{mic} \overset{K_a}{\rightleftarrows} M@(nS)_{mic}, \quad (2)$$

where $(nS)_{mic}$ is a surfactant micelle consisting of several NaDC molecules (the number of NaDC molecules $n > 1$) or a single NaDC molecule ($n = 1$) and $M@(nS)_{mic}$ is a complex dye–surfactant.

Then, to evaluate the binding constants, the dependence similar to the Scatchard equation [25, 26] can be obtained:

$$M_b/(M_0–M_b) = K_a(nS)_0–K_aM_b, \quad (3)$$

where $M_b/(M_0 - M_b)$ is the ratio of the concentrations of dye molecules associated with NaDC (M_b) and unbound dye molecules (M_f) ($M_0 = M_b + M_f$); $(nS)_0$ is the total concentration of micelles ($(nS)_0 = [S]_0/n = (nS)_b + (nS)_f \approx (nS)_f$ under the considered conditions, where $[S]_0$ is the molar surfactant concentration); and K_a is the effective dye–surfactant association constant.

For the binding of the fluorescent *trans*-isomer of the dye, the value of $M_b/(M_0 - M_b)$ can be determined from the fluorescence data:

$$M_b/(M_0–M_b) = (F–F_0)/(F_{max}–F), \quad (4)$$

where F and F_0 are the fluorescence intensities of the dye in the presence and absence of the surfactant, F_{max} is the fluorescence intensity under the condition of binding 100% of the dye molecules (determined graphically from the fluorescence intensity in coordinates $1/F$ versus $1/[S]_0$) [27].

Under the considered conditions $(nS)_0 >> M_0$, then

$$M_b/(M_0–M_b) \approx K_a(nS)_0 = K_a[S]_0/n \quad (5)$$

The experimental dependences obtained from the spectral data for dyes K1 and K2, and the results of their fitting to Eq. (5) are shown in Fig. 6a. The Scatchard plot (Fig. 6a) for the cationic dyes is characterized by the deviation of the experimental points in the regions of low and high NaDC concentrations ($c_{NaDC} \geq$ CMC2). This is mainly due to the formation of dye aggregates at relatively low surfactant concentrations and the interaction of the dyes with secondary micelles at higher surfactant concentrations.

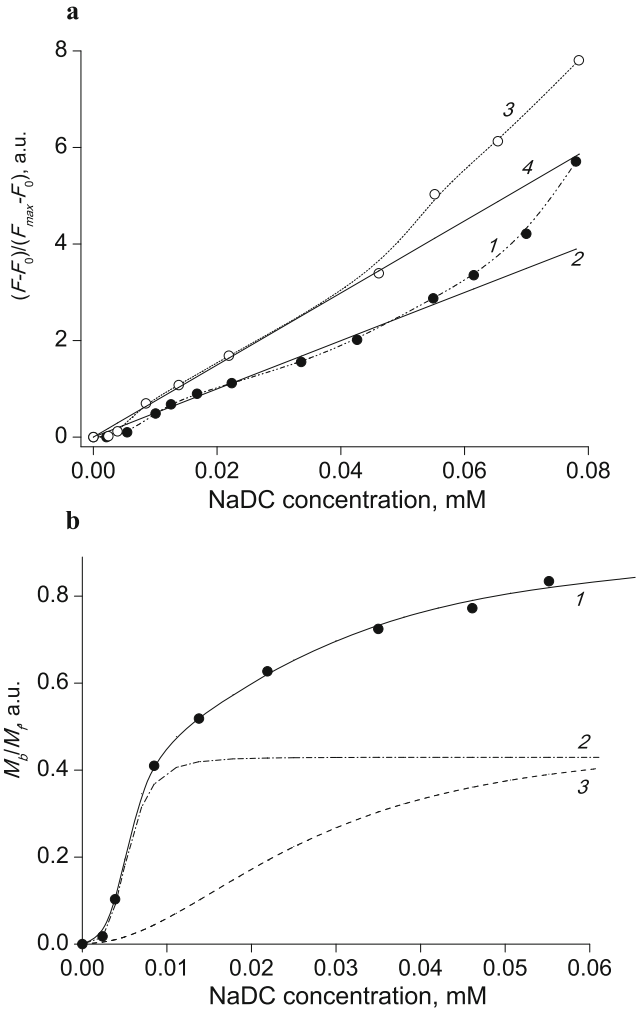

Fig. 6 **a** Plots in the coordinates M_b/M_f versus $[S]_0$ obtained from the fluorescence data for the interaction of dyes (*1*) K1 and (*3*) K2 with NaDC; straight lines (*2*) and (*4*) represent the results of fitting plots to Eq. (5); (**b**) Hill plot (points) obtained for dye K2 (*1*) from fluorescence data in the presence of NaDC and its approximation (line) in the framework of the two-step approach (see text); (*2*, *3*) the results of calculations by Eq. (7) with (*2*) $n = 4$ ($K_{a1} = 1/K_{H1} = 185$ L mol^{-1}) and (*3*) $n = 2$ ($K_{a2} = 1/K_{H2} = 37.3$ L mol^{-1}). The approximation curve *1* was obtained as a sum of the data corresponding to curves *2* and *3*

The values of K_a/n obtained from the slopes of the straight lines given by Eq. (5) (Fig. 6a) are presented in Table 2.

The second model (an analogue of the Hill model [28, 29]) implies the participation of the monomers of dyes K1–K3 and A1 in the formation of associates (micelles) of NaDC upon the interaction with n monomeric surfactant molecules:

$$M + nS \overset{K_a}{\rightleftarrows} M@(nS)_{mic}, \tag{6}$$

where S is a monomeric surfactant molecule, n is the cooperativity coefficient corresponding to the number of surfactant molecules in a dye–surfactant associate

Table 2 Parameters of binding of dye molecules to NaDC micelles (the binding constant for the fluorescent *trans*-isomer K_a, the number of surfactant molecules in a micelle n) in the framework of the Scatchard and Hill models

Dye	K_a/n (Scatchard) L mol^{-1}	K_{a1} (Hill)	K_{a2} (Hill)	n_1	n_2
K1	49.9	123	18.1	4	2
K2	74.7	185	37.3	4	
K3	35.1	179	13.3	3	
A1	10.3	15.8	26.0	6	
A2	~96 (K_{a2}/n)	228	216	6	

$M@(nS)_{mic}$, with $n \geq 1$. Then, to estimate the effective equilibrium constant of the complexation reaction (K_a) of the *trans*-monomers of dyes K1–K3 and A1 with NaDC from the fluorescence data, we can use the Hill equation in the conventional form:

$$\theta = \frac{F - F_0}{F_{max} - F_0} = \frac{S_f^n}{K_H^n + S_f^n} \tag{7}$$

where $\theta = (F - F_0)/(F_{max} - F_0)$ is the portion of binding sites occupied by the dye in the form of a fluorescent *trans*-isomer (determined as earlier from the fluorescence data); S_f is the concentration of unbound surfactant molecules (under the considered conditions, $S_f \approx [S]_0$), K_H is the Hill constant ($K_H = 1/K_a$); n is the Hill coefficient characterizing the cooperativity of binding [28, 29]. The complexity of the equilibrium in the system cationic dyes–NaDC determines the need for using a model with at least two Hill constants (K_{H1}, K_{H2}) and coefficients (n_1, n_2) for accurate fit ($R^2 = 0.995$–0.999) of the fluorescence data. In this model, two dye–surfactant association steps are assumed: the first step (with K_{H1}, n_1), which dominates at lower surfactant concentrations ($[S]_0 < 0.01$ M for K2), and the second step (with K_{H2}, n_2) dominating at higher $[S]_0$ (Fig. 6b). The second step may be attributed to participation of the primary micelles containing dye molecules in the formation of the secondary micelles. The values of K_{a1}, n_1 and K_{a2}, n_2 obtained from the fluorescence data using the Hill equation are given in Table 2.

The anionic thiacarbocyanine dye A2 in aqueous solution is in the form of dimers (D) in equilibrium with *cis*-monomers (M_{cis}) (Eq. (8)), with the equilibrium strongly shifted toward the dimers. Upon the introduction of increasing concentrations of NaDC, we may notice two main stages of the interaction of A2 with the surfactant [15]. At relatively low surfactant concentrations ($[S]_0 < CMC2$), mainly dimers of A2 decompose into *cis*-monomers bound to the surfactant ($M_{cis}@(nS)_{mic}$; Eqs. (8), (9)). At higher surfactant concentrations ($[S]_0 > CMC2$), mainly *cis–trans* conversion of the bound monomers occurs [15]. Then the interaction of A2 with the surfactant at the first stage includes the following processes:

$$2M_{cis} \overset{K_D}{\rightleftarrows} D \quad \left(K_D = [D]/[M_{cis}]^2\right) \tag{8}$$

$$M_{cis} + (nS)_{mic} \overset{K_{a1}}{\rightleftarrows} M_{cis}@(nS)_{mic} \tag{9}$$

Then, denoting the concentration of the dye bound with NaDC micelles as M_b (*cis*-isomer) and the concentrations of free and bound micelles as $(nS)_f$ and $(nS)_b$, and taking into account that $(nS)_f = (nS)_0 - (nS)_b = (nS)_0 - M_b$, (where $(nS)_0$ is the total concentration of micelles) and the concentration of the free dye $M_{cis} = \sqrt{D/K_D}$, in the framework of the Scatchard model [25, 26], we can obtain Eq. (11):

$$M_b/\sqrt{D} = K_{a1}/\sqrt{K_D}\ \left((nS)_0 - M_b\right). \tag{11}$$

Since under the experimental conditions, the concentration of the surfactant is much higher than that of dye A2, we may assume that $(nS)_0 >> M_b$. In this case, Eq. (11) can be rewritten as

$$M_b/\sqrt{D} \approx K_{a1}/\sqrt{K_D}(nS)_0. \tag{12}$$

The equilibrium concentrations of dimers and *cis*-monomers of A2 in aqueous solutions were determined from the absorption spectra using deconvolution of the spectra into Gaussian components—dimer and monomer bands (see [21]). The molar extinction coefficients (ε) for dimers and *cis*-monomers of A2 were determined from changes in the intensities of the bands with changing the concentration of the dye and were found to be 8.06×10^4 and 1.1×10^5 L mol^{-1} cm^{-1}, respectively. With allowance for the found values of ε, after determining the equilibrium concentrations of dimers and *cis*-monomers of A2, the dimerization constant K_D (Eq. (8)) was estimated to be 9.0×10^6 L mol^{-1} at 23 °C. Then from the linear plot of $M_b\sqrt{D}$ versus $[S]_0$ (Eq. (12)), the value of K_{a1}/n was obtained to be ~200 L mol^{-1}.

At the second stage of the interaction of A2 with NaDC ($[S]_0 > CMC2$), *cis*-monomers of A2 bound to micelles are partially converted into *trans*-monomers. This is due to rearrangement of the secondary micelles (probably related to their enlargement) [15]:

$$M_{cis}@(nS)_{mic} + (nS)_{mic} \overset{K_{a2}}{\rightleftarrows} M_{trans}@(nS)_{mic2} \tag{13}$$

The value of $K_{a2}/n \sim 96$ L mol^{-1} was obtained from the fluorescence data ($\lambda_{fl}^{max} = 610$ nm) using Eqs. (4) and (5).

The Scatchard binding constant of the anionic dye A1 was found to be lower than those of the cationic dyes K1–K3 and significantly lower than that of A2. This can be explained by the same charges of dye A1 and the surfactant, which lowers the interaction energy of the dye with the surfactant. The large value of the binding constant of A2 with NaDC is apparently due to its significant hydrophobic properties, which stabilizes the dye in the complex and favors the interaction of A2 with NaDC.

If we use the Hill model (stimulation of micelle formation by the monomeric molecules of A2) [28, 29], Eqs. (6) and (8) will be valid. Denoting the proportion of surfactant micelles occupied by the dye as θ, and the concentration of dye–surfactant associates $(M@(nS)_{mic})$ as M_b ($M_b = K_a \sqrt{D}/\sqrt{K_D}\,[S_0]$, because $(nS)_0 >> M_b$) we can obtain Eq. (14):

$$\theta = M_b/M_0 = M_b/(2D + M_b) = K_a[S_0]^n/\left(2\sqrt{D}/\sqrt{K_D} + K_a[S_0]^n\right). \tag{14}$$

Thus, to estimate the effective equilibrium constant of the complex formation reaction (K_a) A2 with NaDC, the following modification of the Hill equation that takes into account equilibrium (6) and Eqs. (12)–(14) can be applied:

$$\frac{F - F_0}{F_{max} - F_0} = \frac{S_f^n}{K_H^n + S_f^n}\,\frac{\sqrt{K_D}}{2\sqrt{D}} \tag{15}$$

The results of the calculations using Eq. (15) are given in Table 2.

Since the experimental data are fairly well approximated by the Hill model, this may suggest participation of dye molecules in the formation of surfactant micelles (primary and secondary). In the framework of this model, which assumes stimulation of micelle formation by dye molecules, the constants for stimulation by dyes K1–K3 of the formation of primary micelles (K_{a1}) and the Hill coefficients (n_1) are higher than those for secondary micelles (K_{a2}, n_2) (see Table 2). This could be due to a screening effect of the anionic surfactant on the dye cation in primary micelles upon its stimulation of the formation of secondary micelles. For the anionic dyes A1 and A2, which have the same charge as the surfactant, this effect is practically absent, and the values of K_{a1} are close to K_{a2}.

Conclusions

The present work is devoted to a detailed study of the spectral-fluorescent properties of polymethine (carbocyanine) dyes when interacting with sodium deoxycholate, representative of BS. The amphiphilic nature of the molecular structure of BS gives them the ability to carry out transport functions, transfer compounds and ions through biological tissues and membranes. As bio-surfactants, BS play an important role in metabolic processes, drug consumption [30]. Prospects for the use of BS as promising agents for drug delivery [31], encapsulation of biologically active compounds and pharmaceutical

agents [32–34] are being actively studied. The strong dependence of the spectral-fluorescent properties of *meso*-substituted polymethine dyes on the microenvironment permitted us to use such dyes in studies of molecular association of BS in aqueous solutions, the properties of the associates formed, and the interaction of BS molecules and associates with solutes. The present work has shown similarity in the behavior of cationic cyanines upon the interaction with NaDC: aggregate formation at relatively low NaDC concentrations and aggregate decomposition at higher concentrations. For all dyes studied, both cationic and anionic, their binding to BS micelles was observed. This opens up the possibility to encapsulate in BS micelles solutes with different charges. The transformations of the dyes (aggregation–deaggregation, dimer–monomer, *cis–trans*) were observed in the wide range of NaDC concentrations, which reveals changes in the structure and properties of BS associates. With allowance for some approximations, the binding constants of the dyes to NaDC were estimated on the basis of the Scatchard and Hill models. Since the experimental data are fairly well approximated by the Hill model, this may suggest participation of dye molecules in the formation of surfactant micelles.

The pronounced changes in the spectral-fluorescent properties of *meso*-substituted carbocyanine dyes allow us to recommend these dyes as candidates for the role of fluorescent probes to control the formation, structure and properties of bile salt associates (micelles).

Acknowledgements The work was performed under IBCP RAS Russian Federation State Assignment no. 001201253314 (AST and PGP), and under IDB RAS Government Basic Research Program no. 0108-2019-0005 (IGP). Authors thank Prof. B.I. Shapiro and Prof. S.M. Yarmoluk for providing the polymethine dyes.

References

1. Tatikolov AS (2012) Polymethine dyes as spectral-fluorescent probes for biomacromolecules. J Photochem Photobiol C: Photochemistry Reviews 13:55–90. https://doi.org/10.1016/j.jphotochemrev.2011.11.001
2. Kurutos A, Ryzhova O, Trusova V, Gorbenko G, Gadjev N, Deligeorgiev T (2016) Symmetric meso-chloro-substituted pentamethine cyanine dyes containing benzothiazolyl/benzoselenazolyl chromophores novel synthetic approach and studies on photophysical properties upon interaction with bio-objects. J Fluoresc 26:177–187. https://doi.org/10.1007/s10895-015-1700-4
3. Kovalska VB, Losytskyy MY, Yarmoluk SM et al (2011) Mono and trimethine cyanines cyan 40 and cyan 2 as probes for highly selective fluorescent detection of non-canonical DNA structures. J Fluoresc 21:223–230. https://doi.org/10.1007/s10895-010-0709-y
4. Viseu MI, Tatikolov AS, Correia RF, Costa SMB (2014) Time evolution of monomers and aggregates of a polymethine dye probe the dynamics of model vesicles and micelles. J Photochem Photobiol A 280:54–62. https://doi.org/10.1016/j.jphotochem.2014.02.007
5. Atabekyan LS, Chibisov AK (2007) Photoprocesses in aqueous solutions of 9-ethylthiacarbocyanine dyes in the presence of surfactants. High Energy Chem 41:91–96. https://doi.org/10.1134/S0018143907020075
6. Tatikolov AS, Costa SMB (2001) Effects of normal and reverse micellar environment on the spectral properties, isomerization and aggregation of a hydrophilic cyanine dye. Chem Phys Lett 346:233–240. https://doi.org/10.1016/S0009-2614(01)00969-1
7. Tatikolov AS, Costa SMB (2002) Photophysics and photochemistry of hydrophilic cyanine dyes in normal and reverse micelles. Photochem Photobiol Sci 1:211–218. https://doi.org/10.1039/B110450K
8. Carey MC, Small DM (1969) Micellar properties of dihydroxy and trihydroxy bile salts: effects of counterion and temperature. J Coll Interf Sci 31:382–396. https://doi.org/10.1016/0021-9797(69)90181-7
9. Lindman B, Kamenka N, Fabre H, Ulmius J, Wieloch T (1980) Aggregation, aggregate composition, and dynamics in aqueous sodium cholate solutions. J Coll Interf Sci 73:556–565. https://doi.org/10.1016/0021-9797(80)90101-0
10. Li G, McGown LB (1994) Model for bile salt micellization and solubilization from studies of a "polydisperse" array of fluorescent probes and molecular modeling. J Phys Chem 98:13711–13719. https://doi.org/10.1021/j100102a043
11. Matsuoka K, Suzuki M, Honda C, Endo K, Moroi Y (2006) Micellization of conjugated chenodeoxy- and ursodeoxycholates and solubilization of cholesterol into their micelles: comparison with other four conjugated bile salts species. Chem Phys Lipids 139:1–10. https://doi.org/10.1016/j.chemphyslip.2005.08.006
12. Matsuoka K, Moroi Y (2002) Micelle formation of sodium deoxycholate and sodium ursodeoxycholate (part 1). Biochim Biophys Acta 1580:189–199. https://doi.org/10.1016/S1388-1981(01)00203-7
13. Seret A, Bahri M-A (2009) The CMC-like behaviour of bile salts as probed by photoexcited rose Bengal. Colloids and Surfaces A: Physicochem Eng Aspects 339:153–158. https://doi.org/10.1016/j.colsurfa.2009.02.015
14. Mishra SS, Subuddhi U (2014) Spectroscopic investigation of interaction of Nile blue a, a potent photosensitizer, with bile salts in aqueous medium. J Photochem Photobiol B 141:67–75. https://doi.org/10.1016/j.jphotobiol.2014.09.013
15. Tatikolov AS, Pronkin PG, Panova IG (2019) Spectral-fluorescent study of the interaction of polymethine dye probes with biological surfactants – bile salts. Spectrochim Acta Part A: Mol Biomol Spectrosc 216:190–201. https://doi.org/10.1016/j.saa.2019.03.017
16. Tatikolov AS, Pronkin PG (2019) Photochemical processes in molecules of polymethine dye probes in the presence of bile salts. J Appl Spectrosc 85:991–996. https://doi.org/10.1007/s10812-019-00749-w
17. Ishchenko AA (1991) Structure and spectral-luminescent properties of polymethine dyes. Russ Chem Rev 60:865–884. https://doi.org/10.1070/RC1991v060n08ABEH001116
18. Demas JN, Crosby GA (1971) The measurement of photolumineseence quantum yields. A review. J Phys Chem 75:991–1024. https://doi.org/10.1021/j100678a001
19. Akimkin TM, Tatikolov AS, Yarmoluk SM (2011) Spectral and fluorescent study of the interaction of cyanine dyes cyan 2 and cyan 45 with DNA. High Energy Chem 45:222–228. https://doi.org/10.1134/S0018143911030027
20. Kashin AS, Tatikolov AS (2009) Spectral and fluorescent study of the interaction of anionic cyanine dyes with serum albumins. High Energy Chem 43:480–488. https://doi.org/10.1134/S0018143909060113

21. Pelikan P, Ceppan M, Liska M (1994) Applications of numerical methods in molecular spectroscopy, 1st edn. CRC Press, Boca Rarone FL 9780849373220
22. Chibisov AK, Zakharova GV, Görner H (1999) Photoprocesses in dimers of thiacarbocyanines. Phys Chem Chem Phys 1:1455–1460. https://doi.org/10.1039/A809354G
23. Kolesnikov AM, Mikhailenko FA (1987) The conformations of polymethine dyes. Russ Chem Rev 56:275–287. https://doi.org/10.1070/RC1987v056n03ABEH003270
24. West W, Pearce S, Grum F (1967) Stereoisomerism in cyanine dyes-meso-substituted thiacarbocyanines. J Phys Chem 71:1316–1326. https://doi.org/10.1021/j100864a021
25. Scatchard G (1948) The attractions of proteins for small molecules and ions. Ann N Y Acad Sci 51:660–672. https://doi.org/10.1111/j.1749-6632.1949.tb27297.x
26. Nørby JG, Ottolenghi P, Jensen J (1980) Scatchard plot: common misinterpretation of binding experiments. Anal Biochem 102:318–320. https://doi.org/10.1016/0003-2697(80)90160-8
27. Benesi H, Hildebrand J (1949) A spectrophotometric investigation of the interaction of iodine with aromatic hydrocarbons. J Am Chem Soc 71:2703–2707
28. Hill AV (1910) The possible effects of the aggregation of the molecules of hæmoglobin on its dissociation curves. J Physiol 40:iv–vii. https://doi.org/10.1113/jphysiol.1910.sp001386
29. Goutellea S, Maurinc M, Rougierb F et al (2008) The Hill equation: a review of its capabilities in pharmacological modelling. Fundam Clin Pharmacol 22:633–648. https://doi.org/10.1111/j.1472-8206.2008.00633.x
30. Holm R, Müllertz A, Mu H (2013) Bile salts and their importance for drug absorption. Int J Pharm 453:44–55. https://doi.org/10.1016/j.ijpharm.2013.04.003
31. Stojancevic M, Pavlovic N, Golocorbin-Kon S, Mikov M (2013) Application of bile acids in drug formulation and delivery. Front Life Sci 7:112–122. https://doi.org/10.1080/21553769.2013.879925
32. Malik NA (2016) Solubilization and interaction studies of bile salts with surfactants and drugs: a review. Appl Biochem Biotechnol 179:179–201. https://doi.org/10.1007/s12010-016-1987-x
33. Thakur R, Das A, Adhikaria C, Chakraborty A (2014) Partitioning of prototropic species of an anticancer drug ellipticine in bile salt aggregates of different head groups and hydrophobic skeletons: a photophysical study to probe bile salts as multisite drug carriers. Phys Chem Chem Phys 16:15681–15691. https://doi.org/10.1039/C4CP01308E
34. Maity B, Ashique S, Debabrata A, Seth D (2016) Interaction of biologically active flavins inside bile salt aggregates: molecular level investigation. J Phys Chem B 120:854–9866. https://doi.org/10.1021/acs.jpcb.6b04870